Wind Energy Conversion System Using DFIG Controlled by Back-stepping and RST Controller

A. Elmansouri, J. El mhamdi, A. Boualouch
Electrical Engineering Laboratory, ENSET, Mohammed V University in Rabat, Rabat, Morocc

*Abdellatif.elmansouri@um5s.net.ma

Abstract: This paper present a maximum power point tracking (MPPT), the modeling and control backstepping of Double-Fed Induction Generator (DFIG) integrated into a wind energy system. The objective is to apply this technique to control independently the active and reactive power generated by DFIG, and compared with RST controller. The system performance was tested and compared by simulation in terms of following instructions and robustness with respect to parametric variations of the DFIG.

***Keywords**: Back-stepping, Control, DFIG, MPPT, RST Controller, Wind turbine.*

1. INTRODUCTION

The development and use of renewable energy have experienced strong growth in recent years. Among these energy sources, the wind one has a fairly important potential; there is a new solution using alternating machine operating in a rather unusual way; it is the double-fed induction machine (DFIG) [1].

DFIG is very popular because it has certain advantages over all the other variable speed; its use in electromechanical conversion chain as a wind turbine or engine has grown dramatically in recent years [2].Indeed, the energy converter used to straighten and curl alternating currents of the rotor has a fractional power rating of the generator [3], which reduces its cost relative to competing topologies.

In this context, several robust control methods of DFIG appeared; among the backstepping control is one of them. This technique is a relatively new control method for nonlinear systems. It allows sequentially and systematically, by the choice of a Lyapunov function, to determine the system's control law. Its principle is to establish in a constructive manner the control law of the nonlinear system by considering some state variables as virtual Drives and develop intermediate control laws.

2. MAXIMUM POWER POINT TRACKING (MPPT)

2.1. MPPT techniques

In this section, we study the control of a variable speed wind turbine in zone 2 or part load operation with MPPT to technique to ensure greater energy efficiency. This is an operation on wind speeds between 5 m/s and 12 m/s and the pitch angle is constant. For this purpose, we are suggesting the Back-stepping control of the wind turbine to maximize the power extracted. This control strategy is to control the electromagnetic torque (and indirectly the converted electromagnetic power) and to adjust the mechanical speed to its maximum generated electrical power. This principle is known as the Maximum Power Point Tracking terminology.

The priority of this command is to maintain λ to its optimum value $\lambda = \lambda_{opt}$, which provides the value for the power coefficient to be equal to its maximum value. The aim, as with other methods, is therefore to constantly remain in ($\lambda_{opt}, C_{p\max}$). It is therefore possible to vary the turbine rotation speed (Ω_{tur}) according to the wind speed changes. This allows us to continuously work with the optimum aerodynamic efficiency. This is a major advantage of variable speed wind turbines compared with operating at a fixed speed [4].

We get the block diagram of the mechanical speed control shown in the following figure:

978-1-4673-8469-8/16/$31.00

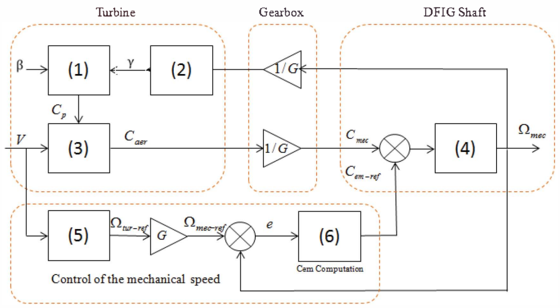

Fig.1: MPPT control with enslavement of speed.

$$C_p = f(\lambda,\beta) = C_1\left(\frac{C_2}{\lambda_i} - C_3\beta - C_4\right)e^{\left(\frac{C_5}{\lambda_i}\right)} + C_6\lambda \tag{1}$$

$$\lambda = \frac{\Omega_{tur}R}{V} \tag{2}$$

$$P_{\max} = \frac{1}{2}C_p(\lambda)\rho.\pi.R^2.v_v^3 \tag{3}$$

$$J\frac{d\Omega_{mec}}{dt} = C_{mec} - C_{em} - f\Omega_{mec} \tag{4}$$

$$\Omega_{tur-ref} = \frac{\lambda_{opt}V}{R} \tag{5}$$

$$C_{em} = K_1K_2\Omega_{mec}^2 - f\Omega_{mec} - J\dot{\Omega}_{mec}^{ref} + Jke \tag{6}$$

2.2. Back-stepping control.

The idea of back-stepping control [5] consists in calculating a control law in order to guarantee that the derivative of Lyapunov function (definite positive) is always negative. First, we calculate the first virtual command from the tracking error (9), this command will be used in the second step as a reference signal for the next state. We repeat the operation until reaching the nth step where we obtain a command that will be applied to the system. In our work, the state vector contains only one variable. So, the synthesis of the back-stepping control law is composed of a single step [6].

$$e = y - y_{ref} \tag{7}$$

The model of the generator shaft is given by the following expression:

$$J\frac{d\Omega_{mec}}{dt} = C_{mec} - C_{em} - f\Omega_{mec} \tag{8}$$

With J, the total inertia of the rotating parts (Kg.m²), f, the coefficient of the viscous damping. C_{em}, the electromagnetic torque of the generator.

$$J = \frac{J_{Turbine}}{G^2} + J_{Generator} \tag{9}$$

According to (2) and:

$$C_{turbine} = \frac{p_m}{\Omega_1} = \frac{1}{2\Omega_1}C_p(\lambda)\rho\pi R^2 v_1^3 \tag{10}$$

$$C_{mec} = \frac{C_{turbine}}{G} \tag{11}$$

$$\Omega_{mec} = G\Omega_{turbine} \tag{12}$$

It is found that: $C_T = K_1K_2\Omega_{mec}^2 - C_{em}$ (13)

Where:

$$K_1 = \frac{0.5\rho\pi R^5}{G^3} \quad (14), \qquad K_2 = \frac{C_p}{\lambda^3} \quad (15)$$

Then the dynamic of the system is given by:

$$\dot{\Omega}_{mec} = \frac{1}{J}\left(K_1K_2\Omega_{mec}^2 - f\Omega_{mec} - C_{em}\right) \tag{16}$$

We have as a reference, $y_{ref} = \Omega_{mec}^{ref}$. The tracking error is given by:

$$e = \Omega_{mec} - \Omega_{mec}^{ref} \tag{17}$$

The time derivative is written:

$$\dot{e} = \dot{\Omega}_{mec} - \dot{\Omega}_{mec}^{ref} = \frac{K_1K_2}{J}\Omega_{mec}^2 - \frac{1}{J}C_{em} - \dot{\Omega}_{mec}^{ref} \tag{18}$$

The Lyapunov function is given by [14]:

$$v(e) = \frac{1}{2}e^2 \tag{19}$$

If this function is always positive definite and its derivative is always negative, then the error will be stable and will tend towards zero. The derivative of the error is given by:

$$\dot{v}(e) = e\dot{e} = e\left(\frac{K_1K_2}{J}\Omega_{mec}^2 - \frac{f}{J}\Omega_{mec} - \frac{1}{J}C_{em} - \dot{\Omega}_{mec}^{ref}\right) \tag{20}$$

A good choice of C_{em} would render $\dot{v}(e)$ negative and ensure the stability of the origin of (20).

Then:

$$\frac{K_1K_2}{J}\Omega_{mec}^2 - \frac{f}{J}\Omega_{mec} - \frac{1}{J}C_{em} - \dot{\Omega}_{mec}^{ref} = -ke,\ (k>0) \tag{21}$$

$$\frac{1}{J}C_{em} = \frac{K_1K_2}{J}\Omega_{mec}^2 - \frac{f}{J}\Omega_{mec} - \dot{\Omega}_{mec}^{ref} + ke \tag{22}$$

$$C_{em} = K_1K_2\Omega_{mec}^2 - f\Omega_{mec} - J\dot{\Omega}_{mec}^{ref} + Jke \tag{23}$$

With this choice, we obtain: $\dot{v}(e) = -ke^2 < 0$.

2.3. Power control by Back-stepping of DFIG.

In this section, we present a new approach to backstepping control applied to the asynchronous machine dual power supply. This approach is designed in such a way to keep the same general structure of a vector control power [7].

Step 1: Computation of the reference rotor currents

We define the errors e_1 and e_2 representing the error between the actual power P_s and the reference power P_{ref} and the error between reactive power Q_s and its reference Q_{ref}.

$$\begin{cases} e_1 = P_{ref} - p_s \\ e_2 = Q_{ref} - Q_s \end{cases} \quad (24)$$

The derivative of this equation gives:

$$\begin{cases} \dot{e}_1 = \dot{P}_{ref} - \dot{P}_s \\ \dot{e}_2 = \dot{Q}_{ref} - \dot{Q}_s \end{cases} \quad (25) \Rightarrow \begin{cases} \dot{e}_1 = \dot{P}_{ref} + V_s \dfrac{M}{L_s} \dot{I}_{qr} \\ \dot{e}_2 = \dot{Q}_{ref} + V_s \dfrac{M}{L_s} \dot{I}_{dr} \end{cases} \quad (26)$$

The first Lyapunov function is chosen sosuch that:

$$v_1 = \frac{1}{2}(e_1^2 + e_2^2) \quad (27)$$

Its derivative is:

$$\dot{v}_1 = e_1 \dot{e}_1 + e_2 \dot{e}_2 \quad (28)$$

$$\dot{v}_1 = e_1(\dot{P}_{ref} - \dot{P}_s) + e_2(\dot{Q}_{ref} - \dot{Q}_s) \quad (29)$$

$$\dot{v}_1 = e_1\left[\dot{P}_{ref} + \frac{MV_s}{L_s}\left(V_{qr} - R_r I_{qr} - g\omega_s \beta I_{dr} - g\frac{MV_s}{L_s}\right)\frac{1}{\alpha}\right] + e_2\left[\dot{Q}_{ref} + \frac{MV_s}{L_s}\left(V_{dr} - R_r I_{dr} - g\omega_s \beta I_{qr}\right)\frac{1}{\alpha}\right]$$
(30)

The pursuits of goals are achieved by choosing the references of the current components representing the stabilizing functions as follows:

$$\begin{cases} I_{qrref} = X\left[k_1 e_1 + \dot{P}_{ref} + \dfrac{V_s M}{L_s \alpha}\left(V_{qr} - g\omega_s \beta I_{dr} - g\dfrac{MV_s}{L_s}\right)\right] \\ I_{drref} = X\left[k_2 e_2 + \dot{Q}_{ref} + \dfrac{V_s M}{L_s \alpha}\left(V_{dr} + g\omega_s \beta I_{qr}\right)\right] \end{cases} \quad (31)$$

With: $X = \dfrac{L_s \alpha}{V_s M R_r}$, $\beta = L_s - \dfrac{M^2}{L_s}$, $\alpha = L_r - \dfrac{M^2}{L_s}$

Where: k_1, k_2: positive constants.

The derivative of the Lyapunov function becomes:

$$\dot{v}_1 = -k_1 e_1^2 - k_2 e_2^2 \quad (32)$$

So, I_{qrref} and I_{drref} in (31) are asymptotically stable.

Stepe2: computation of the control voltages.

We define the errors e_3 and e_4 respectively representing the error between the current quadrature rotor I_{qr} and the reference current I_{qrref} and the error between the direct rotor current I_{dr} and I_{drref} reference.

$$\begin{cases} e_3 = I_{qrref} - I_{qr} \\ e_4 = I_{drref} - I_{dr} \end{cases} \quad (33)$$

The derivative of this equation gives:

$$\begin{cases} \dot{e}_3 = \dot{I}_{qrref} - \dot{I}_{qr} \\ \dot{e}_4 = \dot{I}_{drref} - \dot{I}_{dr} \end{cases} \quad (34) \Rightarrow \begin{cases} \dot{e}_3 = \dot{I}_{qrref} - \dfrac{1}{\alpha} V_{qr} - S_1 \\ \dot{e}_4 = \dot{I}_{drref} - \dfrac{1}{\alpha} V_{dr} - S_2 \end{cases} \quad (35)$$

With:

$$S_1 = \frac{1}{\alpha}\left(R_r I_{qr} - g\omega_s \beta I_{dr} - g\frac{MV_s}{L_s}\right) \quad (36)$$

$$S_2 = \frac{1}{\alpha}\left(-R_r I_{dr} + g\omega_s \beta I_{qr}\right) \quad (37)$$

Actual control laws of the machine V_{qr} and V_{dr} shown in (35), then we can go to the final step.

The final Lyapunov function is given by:

$$v_2 = \frac{1}{2}(e_1^2 + e_2^2 + e_3^2 + e_4^2) \quad (38)$$

The derivative of equation is given by:

$$\dot{v}_2 = e_1 \dot{e}_1 + e_2 \dot{e}_2 + e_3 \dot{e}_3 + e_4 \dot{e}_4 \quad (39)$$

Which can be rewritten as follows:

$$\begin{aligned} \dot{v}_2 &= -k_1 e_1^2 - k_2 e_2^2 - k_3 e_3^2 - k_4 e_4^2 \\ &+ e_3\left(k_3 e_3 + \dot{I}_{qrref} - \frac{1}{\alpha} V_{qr} - S_1\right) \\ &+ e_4\left(k_4 e_4 + \dot{I}_{drref} - \frac{1}{\alpha} V_{dr} - S_2\right) \end{aligned} \quad (40)$$

Where: k_3, k_4 Positive constants.

Control voltages V_{qr} and V_{dr} are selected as:

$$\begin{cases} V_{qr} = \alpha\left(k_3 e_3 + \dot{I}_{qrref} - S_1\right) \\ V_{dr} = \alpha\left(k_4 e_4 + \dot{I}_{drref} - S_2\right) \end{cases} \quad (41)$$

Which ensures : $\dot{v}_2 < 0$

The stability control is obtained by a good choice of gains: k_1, k_2, k_3 and k_4.

The general structure of control by the backstepping of DFIG is illustrated in Figure (2) the blocks computation I_{qrref} and I_{drref} represent the fictitious control, respectively provide current references obtained from the errors of active and reactive power.

The computation of commands voltages V_{qr} and V_{dr} are based on the error between the currents references and actual implanted by equation (41)

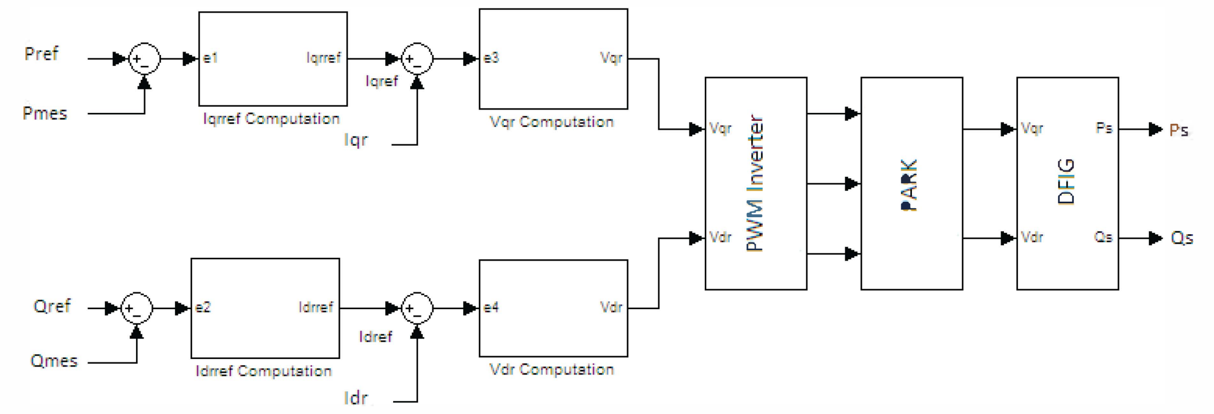

Fig.2: Block diagram of the control with power loop

2.4. RST Controller Synthesis:

The RST controller is composed of three polynomials R, S and T. The determination of strategy of the three polynomial allows performance tuning of the servo with the synthesis parameters T_c (control horizon) and T_f (filtering horizon) [8].

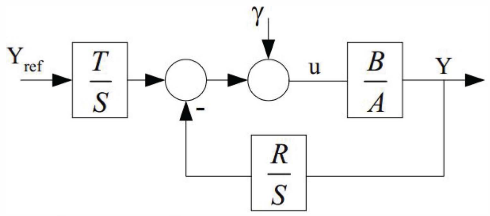

Fig.3 Block diagram of the RST controller.

A and B are respectively the denominator and the numerator of the transfer-function of the system, Y_{ref} isthe reference and γ is the disturbance. In our case:

$$A = L_s R_r + pL_s(L_r - \frac{L_m^2}{L_s}) \text{ And } B = L_m V_s \quad (42)$$

The transfer-function of the regulated system is:

$$Y = \frac{BT}{AS+BR} Y_{ref} + \frac{BS}{AS+BR}\gamma \quad (43)$$

To determine S (p) and R (p) we specified an arbitrary stability polynomial D (p), calculated according to the Bezout equation: D = AS + BR with:

$$\deg(D) = \deg(A) + \deg(S) \quad (44)$$

For the proposed model, we have:

$$A = a_1 p + a_0$$
$$B = b_0$$
$$D = d_3 p^3 + d_2 p^2 + d_1 p + d_0 \quad (45)$$
$$S = s_2 p^2 + s_1 p + s_0$$
$$R = r_1 p + r_0$$

With the strategy of robust pole placement, the polynomial D is written as:

$$D = CF = (s + \frac{1}{T_c})(s + \frac{1}{T_f})^2 \quad (46)$$

With:

C: Command polynomial

F: Filter polynomial

T_c :Control horizon

T_f: Filtering Horizon

And:

$P_c = -\frac{1}{T_c}$ Is pole of polynomial C.

$P_f = -\frac{1}{T_f}$ Is double pole of the polynomial F.

In order to accelerate the system we chose P_A far exceeds P_c.

$$p_c = 5 p_A = -5 \frac{L_s R_r}{L_s(L_r - \frac{L_m^2}{L_s})} \quad (47)$$

To make the control less sensitive to noise and therefore make the most robust control setting $T_c > 3T_f$

$$T_f = \frac{1}{3} = \frac{L_s(L_r - \frac{L_m{}^2}{L_s})}{5\,L_s R_r} \qquad (48)$$

From equation 46, 47 and 48, we deduce the coefficients of polynomial D which are linked to the coefficients of S and R by the Sylvester matrix [11]. Thus, we can determine the parameters of the RST controller as follows:

$$\begin{cases} d_3 = a_1 s_2 \\ d_2 = a_1 s_1 \\ d_1 = a_0 s_1 + b_0 r_1 \\ d_0 = b_0 r_0 \\ T = r_0 \end{cases} \Longrightarrow \begin{cases} s_2 = \dfrac{d_3}{a_1} \\ s_1 = \dfrac{a_1}{s_1} \\ r_1 = \dfrac{d_1 - a_0 s_1}{b_0} \\ r_0 = \dfrac{d_0}{b_0} \end{cases} \qquad (49)$$

3. System Overview

The turbine that we will study is a 10 KW wind turbine. It is a three-bladed horizontal axis model, the length of a blade is 3.5m and the speed multiplier ratio is 5.8.

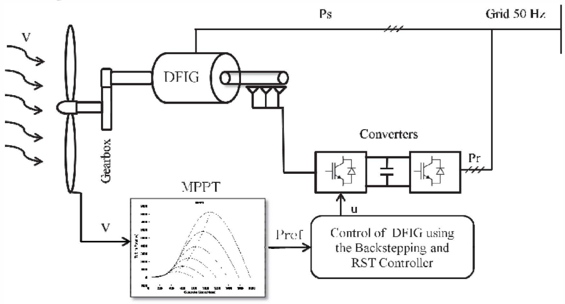

Fig.4 Control structure of DFIG in WECS.

3.1. Modeling of the wind turbine:

The total kinetic power available on a wind turbine is given by [9]:

$$P_{\max} = \frac{1}{2}\rho S v_v^3 = \frac{1}{2}\rho\pi R^2 v_v^3 \qquad (50)$$

The aerodynamic power is given by:

$$P_{\max} = \frac{1}{2} C_p(\lambda)\rho.\pi.R^2.v_v^3 \qquad (51)$$

$$C_p = f(\lambda,\beta) = C_1\left(\frac{C_2}{\lambda_i} - C_3\beta - C_4\right)e^{\left(\frac{C_5}{\lambda_i}\right)} + C_6\lambda \qquad (52)$$

With:

$$C_{turbine} = \frac{p_m}{\Omega_1} = \frac{1}{2\Omega_1} C_p(\lambda)\rho\pi R^2 v_1^3 \qquad (53)$$

$$P_{mg} = C_p P_m = \frac{1}{2} C_p\left(\frac{R\Omega_2}{KV_1}\right)\rho\pi R^2 v_1^3 \qquad (54)$$

$$\frac{1}{\lambda_i} = \frac{1}{\lambda + 0.08\beta} - \frac{0.035}{\beta^3 + 1} \qquad (55)$$

Multiplier model:

$$C_{mec} = \frac{C_{turbine}}{G} \qquad (56)$$

Model of the shaft:

The fundamental equation of dynamics can be written [9]:

$$J\frac{d\Omega_{mec}}{dt} = C_{turbine} - f\Omega_{mec} \qquad (57)$$

With: $\Omega_{mec} = G\Omega_{turbine}$ (58)

$$J\frac{d\Omega_{mec}}{dt} = C_{mec} - C_{em} - f\Omega_{mec} \qquad (59)$$

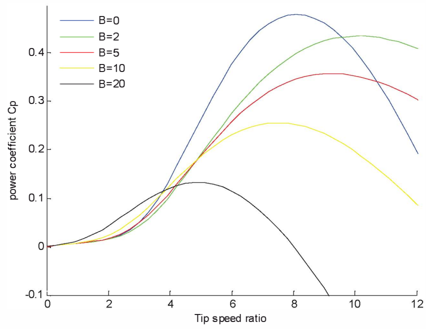

Fig.5: Power coefficient $C_p(\lambda,\beta)$

The figure (5) shows the C_p curves for multiple values of β. This curve is characterized by the optimum point; this value is called the Betz limit.

4. Modeling of the DFIG

The model of DFIG is equivalent to the model of the induction machine cage. However, the rotor of the DFIG is not shorted [10].

Park transformation:

The classical electrical equations of the DFIG in the Park frame are written as follows [11]:

$$\begin{cases} V_{sd} = R_s I_{sd} + \dfrac{d\phi_{sd}}{dt} - \dot{\theta}_s\,\phi_{sq} \\ V_{sq} = R_s I_{sq} + \dfrac{d\phi_{sq}}{dt} - \dot{\theta}_s\,\phi_{sd} \end{cases} \qquad (60)$$

$$\begin{cases} V_{rd} = R_r I_{rd} + \dfrac{d\phi_{rd}}{dt} - \dot{\theta}_s\,\phi_{rq} \\ V_{rq} = R_s I_{rq} + \dfrac{d\phi_{rq}}{dt} - \dot{\theta}_s\,\phi_{rd} \end{cases} \qquad (61)$$

The stator and rotor flux can be expressed as:

$$\begin{cases} \phi_{ds} = L_s i_{ds} + MI_{dr} \\ \phi_{qs} = L_s i_{qs} + MI_{qr} \end{cases} \qquad (62)$$

$$\begin{cases} \phi_{dr} = L_r i_{dr} + MI_{ds} \\ \phi_{qr} = L_s i_{qr} + MI_{qs} \end{cases} \qquad (63)$$

The electromagnetic torque is given by the following expression:

$$C_{em} = P\frac{M}{L_s}(\phi_{ds} I_{qr} - \phi_{qs} I_{dr}) \qquad (64)$$

Mechanical Equation:

$$\frac{d\Omega}{dt} = \frac{1}{J}(C_{em} - C_r - f_r\Omega) \quad (65)$$

$$C_{em} = P[I_s]^T + \frac{d}{d\theta}([M_{sr}][I_r]) \quad (66)$$

The previous equations used to establish a block diagram of the electrical system to regulate:

5. SIMULATIONS RESULTS:

The Control of The DFIG proposed was simulated using (Matlab / Simulink). The parameters of the DFIG [12] are attached. The parameters k_1, k_2, k_3 and k_4 of backstepping control are chosen as follows: $k_1 = 80600$, $k_2 = 900600$, $k_3 = 5000$, $k_4 = 6000$, $k = 0.001$ to meet the convergence condition.

In this article we present the response of the DFIG under the backstepping, and the RST controller, the following figures illustrate the active and reactive power with change of parameters (Rr, Ls, Lr).

The machine speed is attached to 1450 rpm in ideal conditions, the active power reference P_{ref} is 5KW and 10KW. The reactive power reference Q_{ref} is 0 Var. Figure (6) and (7) shows the response of active and reactive power by the RST and Backstepping controller.

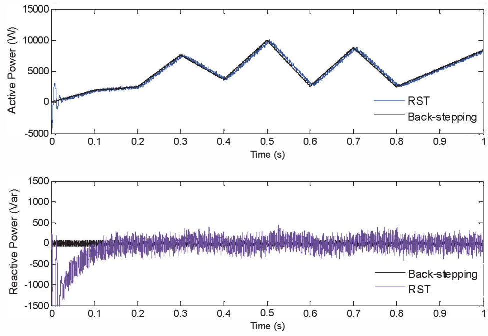

Fig.6: Response to the active and reactive power using RST and Backstepping controller when wind speed varies approximately to real conditions

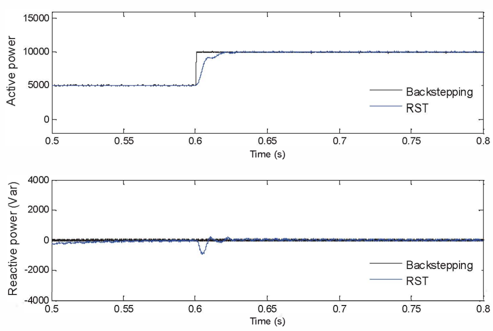

Fig.7: Response to the active and reactive power using RST and Backstepping controller when step change of wind speed

From the figure, we can conclude that the stator active and reactive power P_s and Q_s follow the reference grandeur P_{ref} and Q_{ref}. We note a quicker response for the Backstepping controller and an exceeded for RST controller. To guarantee a unity power factor at the stator side, the reactive power is maintained to zero (Qsref=0)

Robustness test:

The parameters of the system are subject to changes driven by different physical phenomenal, so our controller should provide good control whatever the variation of the generator parameters. In order to test the robustness of the controller we varied the rotor resistance R_r to $2R_r$, and the inductance value of the rotor and stator 10% from its nominal value. Figures 5, 6 and 7respectively show the effect of varying the parameters of the generator R_r, L_s and L_r on the response of the active and reactive power.

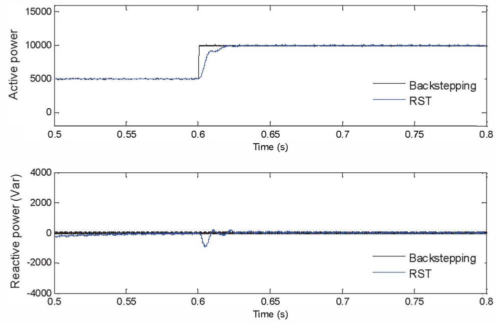

Fig. 8: Active and reactive power with R_r variation ($2R_r$)

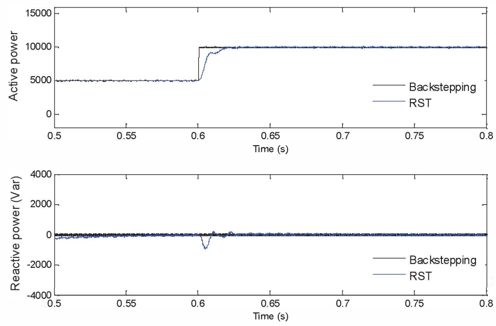

Fig.9: Active and reactive power with L_s variation(10%)

From simulation results, we found that the Back-stepping controller is more robust, the response time is almost the same despite changes in the parameters of the DFIG.

6. CONCLUSION

The first part of this article is devoted to the design of a backstepping control law for DFIG. This law is established step by step while ensuring the stability of the loop machine closed by a suitable choice of the Lyapunov function.

The second part presents the RST controller which comprises of three polynomials R, S and T. The determination of strategy of the three polynomial allows performance tuning of the servo with the synthesis parameters Tc (control horizon) and Tf (filtering horizon).

The three part presents the modeling of the turbine and controlling of the machine based on the physical equations, followed by simulation of operation.

In the end the simulation result allows us to show the proposed algorithm capabilities, in terms of regulation, tracking and disturbance rejection, and demonstrating the robustness of this technique can advantageously replace conventional RST control.

7. RÉFÉRENCES

[1] E. Tremblay, S. Atayde , A. Chandra,'' Direct Power Control of a DFIG-based WECS with Active Filter Capabilities'' Electrical Power & Energy Conference (EPEC), pp. 1-6 . October 2009.

[1] Nihel KHEMIRI, Adel KHEDHER, Mohamed Faouzi MIMOUNI3,''An Adaptive Nonlinear Backstepping Control of DFIG Driven by Wind Turbine'' WSEAS TRANSACTIONS on ENVIRONMENT and DEVELOPMENT, Issue 2, Volume 8, April 2012.

[2] K. KERROUCHE, IEEE, A. MEZOUAR, L. BOUMEDIEN, "A Simple and Efficient Maximized Power Control of DFIG Variable Speed Wind Turbine", the 3rd International Conference on Systems and Control, Algeria, pp. 29-31, October 2013.

[3] S. S. GE, C. WANG and T. H. LEE "ADAPTIVE BACKSTEPPING CONTROL OF A CLASS OF CHAOTIC SYSTEMS". International Journal of Bifurcation and Chaos, Vol. 10, No, pp.1149-1156, 2000.

[4] Nihel KHEMIRI, Adel KHEDHER, Mohamed Faouzi MIMOUNI, ''Wind energy conversion system using DFIG controlled by Backstepping and sliding mode strategies '' International journal of renewable energy research, Volume 2, No.3, 2012

[5] Xie Zhen, Zhang Xing, Yang Shuying, Li Qin, ZhaiWenfeng, ''Study on Control Strategy of Maximum Power Capture For DFIG in Wind Turbine System'', Power Electronics for Distributed Generation Systems, pp. 110-115, 2010.

[6] A. Mechtar, K. Kemh, M. Ghanes, ''Power Control for High speed Wind by Using the Backstepping Strategy '' 2nd International Symposium on Computer, Communication, Control and Automation (3CA 2013), April 2012.

[7] Nihel KHEMIRI, Adel KHEDHER, Mohamed Faouzi MIMOUNI, ''An Adaptive Nonlinear Backstepping Control of DFIG Driven by Wind Turbine'' WSEAS TRANSACTIONS on ENVIRONMENT and DEVELOPMENT, pp.2224-3496, Issue 2, Volume 8, April 2012.

[8] A.Belabbes, B.Hamane, M. Bouhamida, A.Draou,"Power Control of a Wind Energy Conversion System based on a Doubly Fed Induction Generator using RST and Sliding Mode Controllers" ,*International Conference on Renewable Energies and Power Quality*, Santiago de Compostela-Spain, March, 2012

[9] F. Poitiers, M. Machmoum, R. Le Doeuff, M.E. Zaim, "Control of a doubly-fed induction generator for wind energy conversion systems",*International Journal of Renewable Energy Engineering*, Vol. 3, N° 3, December 2001, pp. 373–378.

[10] B. Beltran, T. Ahmed-Ali, M.E.H. Benbouzid, "Sliding mode power Control of variable speed wind energy conversion systems," , Electric Machines & Drives Conference, (IEMDC)., vol.23, no.22, pp.551–558, Jun.2008.

[11] Kouadria Selman, BelfedhalSeifeddine, MesslemYoucef, Berkouk El Madjid, ''Study and control of wind energy conversion system(WECS) based on the doubly fed induction generator(DFIG) connected to the grid'',Ninth International Conference on Ecological Vehicles and Renewable Energies (EVER), pp.1-7, 2014.

[12] A. Elmansouri, J. El mhamdi, A. Boualouch, " Control by Back Stepping of the DFIG Used in the Wind Turbine." , International Journal of Emerging Technology and Advanced Engineering IJETAE, Volume 5, Issue 2, pp 472- 478, February 2015.

8. APPENDIX

Table 1:Wind turbine data

Blade Radius	R=3 m
Base wind speed	12 m/s
Power coefficient	0.48
Optimal relative wind speed	8.1

Table 2: DFIG parameters

Rated power	10kw
Rated stator voltage	Vs=220V
Nominal frequency	Ws=2π50
Number of pole pairs	P=2
Rotor resistance	Rr=0.62Ω
Stator resistance	Rs=0.455Ω
Stator inductance	Ls=0.084 H
Rotor inductance	Lr=0.085 H
Mutual inductance	M=0.078 H
Sliding	g=-0.03

Power coefficient constants:

$c_1 = 0.5176, c_2 = 116, c_3 = 0.4, c_4 = 5, c_5 = 21,$

$c_6 = 0.0068$

Packstepping parameters:

$k_1 = 80600$, $k_2 = 900600, k_3 = 5000$, $k_4 = 6000$

$k = 0.001$

$P_{ref} = 10Kw\ Q_{ref} = 0VAr$

List of symbols:

ρ : Air density

R :Blade radius.

v_v : Wind speed (m/s)

$P_{\max}$: Wind maximum power.

C_p: Power coefficient:

$\lambda = \frac{\Omega_1 R}{V_1}$: Relative wind speed

Ω_1 : Wind turbine speed(Shaft speed).

C_{mec} : Wind turbine torque (Nm).

G : Mechanical speed multiplier.

Ω_{mec}: Mechanical speed (rad/s).

P_{mg} : Mechanical power (watts).

Ω_2: Rotation speed multiplier (rad/s).

f : Damping coefficient.

C_{em} : Electromagnetic torque(Nm).

J : Moment of inertia(Kg.m²)

V_{dr}, V_{qr} : Direct and quadrature rotor voltages

$C_{turbine}$: Wind turbine torque (Nm)